

HRR 00855

Current source density analysis of frequency coding in the inferior colliculus *

David M. Harris

*Dept. of Otolaryngology-Head and Neck Surgery, Eye & Ear Infirmary, University of Illinois, College of Medicine at Chicago,
1855 West Taylor Street, Chicago, IL 60612, U.S.A.*

(Received 11 October 1985; accepted 24 August 1986)

Current source density (CSD) analysis is a technique that provides information about the time course and spatial location of transmembrane currents derived from a laminar collection of evoked potentials. Restrictive conditions for acquisition of evoked potentials are required in order to yield a one-dimensional CSD analysis that is an accurate estimate of synaptic activity. Satisfaction of these conditions was assumed in recordings of tone-burst-evoked potentials along the axis of symmetry (tonotopic) in the inferior colliculus of adult mongolian gerbils. Off-line these data were converted into distance/voltage functions. The second spatial derivatives of these functions gave a family of profiles of the spatial distribution of current source and sink densities at discrete latencies relative to the stimulus. Results indicate a frequency-dependent spatial shift in the evoked current sink of about 280 μm octave. This sink, indicative of local excitatory synaptic drive, is surrounded, both spatially and temporally, by current sources. The spatial extent of excitation as estimated from CSD analysis, compares well quantitatively with predictions from an across-neuron model that is based on single unit data.

inferior colliculus, frequency coding, neuronal ensemble, current source density

Introduction

Volume-conducted gross potentials (e.g., auditory brainstem response, E.E.G., etc) are indirect measures of neuronal activity (Purpura, 1959; Creutzfeldt et al., 1966, 1969; Elul, 1964, 1974; Gerstein, 1970; John, 1972). Interpretation of these potentials is hampered by the uncertainty in identifying the underlying generators. Current source density (CSD) analysis may aid gross potential analysis by extracting information about local transmembrane activity (Lorente de No, 1947; Pitts, 1952; Howland et al., 1955; Nicholson and Llinas, 1971). Under certain circumstances the location and time course of synaptically generated sources and sinks can be calculated from a spatial profile of extracellular voltages. The slope of this

profile or first derivative of the function represents current flow. The curvature of the space/voltage function, the second derivative, represents the density of current sources and sinks, indicative of transmembrane currents induced by local activity.

Previous work has substantiated the ability of CSD analysis to precisely localize the sites of synaptic interactions and to disclose principles of organization not accessible to other methods. This analytic technique has been developed, applied and tested in the cerebellum where there is a high degree of spatial order (Nicholson and Llinas, 1971; Freeman and Nicholson, 1975; Nicholson and Freeman, 1975). CSD analysis has also been applied extensively to the study of the synaptic organization of the visual pathway where results both parallel and augment findings derived from conventional intracellular, single unit and anatomic techniques (Mitzdorf and Singer, 1977, 1979, 1980; Freeman and Singer, 1983).

CSD analysis is also suited to study spatial

* Preliminary results have been reported in abstract (Harris and Rosenfeld, 1975; Harris and Riera-March, 1985). Supported by NIH-NINCDS NS19518-03 and The Deafness Research Foundation.

coding of sensory information. A spatial code is identified when a systematic change in the stimulus produces a systematic change in the spatial pattern of active elements (Perkel and Bullock, 1968). In this regard, CSD analysis can provide a spatial profile of synaptic input related to the patterns of extracellular voltages.

The general form of the CSD equation is a derivation of the Poisson equation for potentials in a volume conductor:

$$I_m(x, y, z) = - \left(\frac{\partial^2 \Phi}{\partial x^2} \sigma_x + \frac{\partial^2 \Phi}{\partial y^2} \sigma_y + \frac{\partial^2 \Phi}{\partial z^2} \sigma_z \right) \quad (1)$$

where,

$I_m(x, y, z)$, current source density;
 $\sigma_x, \sigma_y, \sigma_z$, components of conductivity;
 Φ , field potential.

We use a special case of this equation for analyses of tone-burst-evoked CSD profiles in one dimension along an electrode penetration. This technique was also used by Muller-Preus and Mitzdorf (1984) for the cat inferior colliculus (IC) using click stimuli and by Manis and Brownell (1983) for cat dorsal cochlear nucleus using electrical VIIIth nerve stimulation. A one-dimensional analysis is justified by one fundamental assumption: that there is negligible current flow perpendicular to the path of the recording electrode. In order for this assumption to be valid, three conditions must be satisfied:

1. There must be an inherent geometric symmetry of the region being measured and measurements are made along an axis of symmetry.
2. Elements within the region must be activated synchronously.
3. The region must have a fairly homogeneous conductivity.

The satisfaction of these conditions ensures that areas contiguous to the recording sites are at negligible potential differences at matching points in time. Negligible potential differences over regions of similar conductivities give negligible cur-

rent flow perpendicular to the axis of the one-dimensional analysis. This allows one to assume that the partial differentials of the y and z components of Eqn. 1 are equal to zero.

In the central nucleus of the IC these conditions appear to be satisfied. Anatomical structure, single unit spatial reconstructions and 2-deoxyglucose uptake studies define a laminar organization related to frequency encoding (Aitkin et al., 1975; Clopton and Winfield, 1973; Merzenich and Reid, 1974; Rockel and Jones, 1972; Rose et al., 1963; Roth et al., 1978; Ryan et al., 1982). A tonotopic sequence exists along an axis of symmetry and it seems reasonable that frequency-specific lamina are activated synchronously. Muller-Preus and Mitzdorf (1984) pointed out that the uniform distribution of neurons characteristic of the central nucleus lends credence to the assumption of homogeneous conductivity. Given the above assumptions, a one-dimensional CSD analysis should provide an accurate description of the distribution of current sources and sinks evoked along the tonotopic axis by tone-burst stimuli.

Methods

Adult mongolian gerbils were anesthetized initially with pentobarbital (Nembutal, 50 mg/kg, i.p.) plus ketamine (20 mg/kg, i.m.), and a tracheal cannula was inserted. Anesthesia was maintained with ketamine (10 mg/kg per h). The right osseous external auditory meatus was exposed to permit coupling of the sound system and a small hole was made in the lateral wall of the meatus to accommodate a microphone probe tube. A silver wire was placed in the round window niche for monitoring the compound action potential (AP) of the auditory nerve. Portions of the parietal and occipital bones were removed to provide access to the left IC. Heart rate, respiration rate and core temperature were monitored to assure that the data were acquired while these parameters were within normal limits.

A PDPII/23 + computer controlled stimulus frequency (Tektronics FG 502 Voltage controlled oscillator), level (Shiba-Soku 528-3) and timing (Wilsonics BSIT cosine electronic switch; see Fig. 1 for timing variables). Sound, produced by a TDH49 earphone, was delivered through a 3 cm

exponential horn sealed to the external meatus. Sound pressure levels (re 20 μP) were estimated from the corrected RMS voltage output of a Brüel & Kjaer 4170 $\frac{1}{2}$ inch probe tube microphone.

Compound action potential thresholds were obtained for tone-bursts with carrier frequencies from 250 Hz to 20 kHz. Thresholds were collected periodically to evaluate the stability of the sound and the peripheral auditory systems. Sound levels used in these experiments are expressed re AP threshold.

An incision was made in the dura along the sulcus between cerebellum and transverse sinus, and the dorsal pole of the left IC was visualized after slight retraction of the sinus. A microelectrode was positioned at the IC surface 1.5–2.0 mm lateral to the midline and angled to traverse the long axis in the sagittal plane (Fig. 4). The exposed surface of the brain was covered with an insulating layer of mineral oil. Monopolar recordings were made with tungsten microelectrodes (Diamond) having impedances of 1–5 $\text{M}\Omega$, referenced to a needle electrode in the snout. Signals were sensed by a WPI 750 Microprobe headstage and amplifier, band-pass filtered between 10 and 800 Hz (Grass P15), monitored and digitized (Data Translation A/D Converters, sample rate = 6.4 kHz). The electrode was advanced remotely (Trent Wells hydraulic) and tone-burst-evoked field potentials were collected at 100 μm increments and stored on disk. For the experiments reported here, 50 ms tone-burst stimuli (2 ms rise–decay) with six frequency and level combinations, 0.625, 2.50, and 10.0 kHz at 20 and 40 dB above AP threshold, were presented. Averaged evoked potentials ($N = 200$) were acquired at each increment along a 4–5 mm electrode trajectory (e.g., 5 mm = 50 recording locations). Results are reported from seven animals in which this entire protocol was completed successfully.

A one-dimensional CSD analysis was performed off-line using a finite difference formula for evaluation of the second derivative. A seven point smoothing algorithm (Pitts, 1952) was used in order to attenuate higher frequency noise across the spatial dimension. The substitution of a three point finite difference function did not affect the relative location of the peaks of the source and sink densities.

At the end of each experiment, animals were injected with 100 mg/kg of barbiturate and perfused with normal saline followed by buffered 10% formalin plus 5% methylene blue. Heads remained in formalin for at least 48 h, then the bone was decalcified in 1% nitric acid until radiolucent. As frozen sections of the skull and brain were made (50 μm) the cut surface was photographed from above. Sections were mounted and stained with thionin. The film strip of serial sections was processed with a graphics system that allowed precise in situ reconstructions.

Results

Fig. 1 illustrates the off-line transformations performed on a collection of averaged evoked potential waveforms to produce a space-time map. The plot labeled 'Evoked potentials' represents the averaged potentials evoked by a 2.5 kHz tone-burst of 50 ms duration at 20 dB above AP threshold. The waveforms are arranged according to the recording locations along a 4.0 mm penetration. Even in this form it is obvious that a localized response is evoked between 1.5 and 2.5 mm. The following transformations enhance our ability to localize this response and provide information on local transmembrane currents.

A software analysis program determines the voltages at a specific latency within each evoked potential waveform and compiles a distance voltage function, $V = F(x)$. A family of functions arranged according to time (1.25 ms intervals) is shown in Fig. 1, 'Voltages.' In this illustration the functions have been smoothed with a seven point Hamming window (Hamming, 1962; Freeman and Nicholson, 1975), and the surfaces have been rotated and plotted with a hidden line routine to produce the illusion of three dimensions. A widespread onset response can be seen across the top of the plot. This is followed by a more localized negativity ($-120 \mu\text{V}$ minimum) and an offset response ($40 \mu\text{V}$), both centered at 1.8 mm.

The first derivative, $F'(x) = dV/dx$, is computed to find the slope of $V = F(x)$ for each latency. The family of the first spatial derivatives is plotted in Fig. 1 ('Current Flow Density'). At this stage we have, in essence, the same result as a series of bipolar recordings obtained with a tip

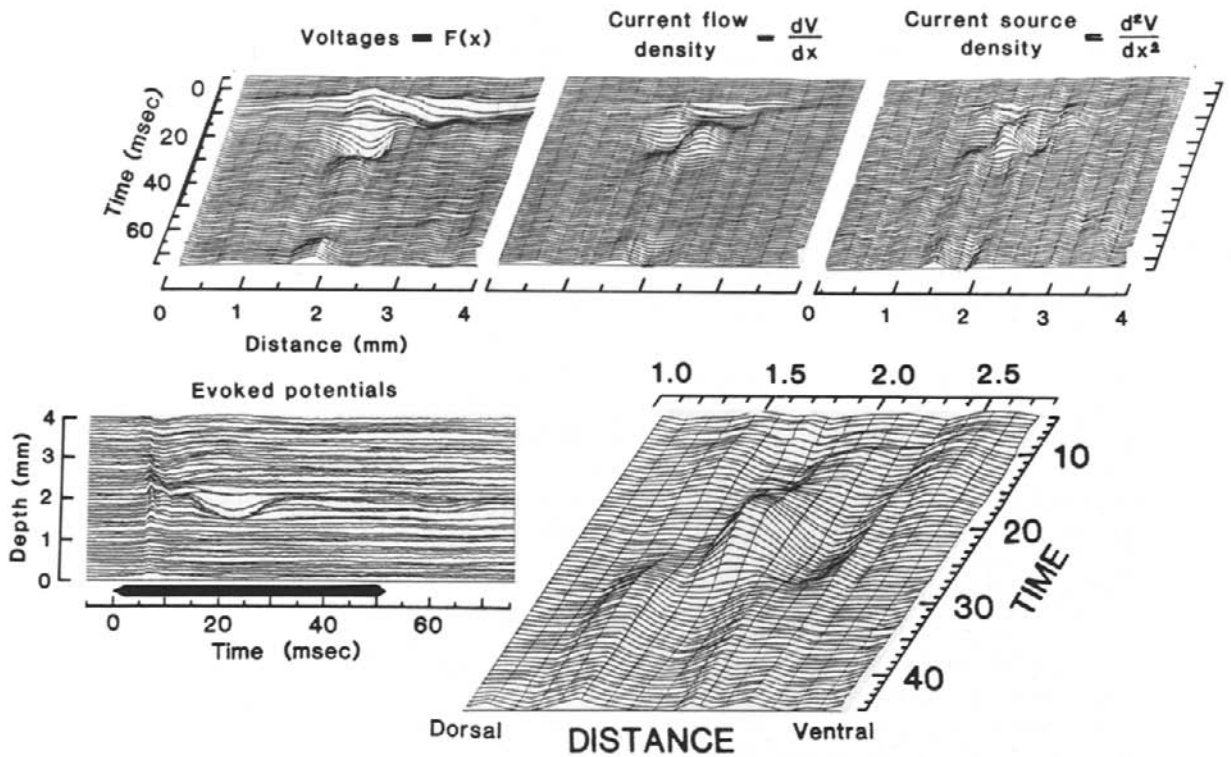


Fig. 1. Graphic description of CSD analysis in the inferior colliculus of an adult gerbil. Lower left: Raw data were collected as a series of averaged evoked potentials ($N = 200$) measured at $100 \mu\text{m}$ increments along a 4.0 mm electrode trajectory (see Fig. 4 for electrode track). Tone-burst stimulus: 2.5 kHz at 20 dB above threshold of the auditory nerve response, 2 ms cosine rise-decay, 50 ms duration, 5/s repetition rate. Responses are acquired within an 80 ms window. The window is divided into a 5 ms pre-stimulus interval, a 50 ms stimulus interval and a 25 ms post-stimulus interval. Upper left to right: The data are resorted to produce smoothed, voltage/distance functions from the raw, voltage/time potentials. The first spatial derivative (current flow density) and the second spatial derivative (current source density) illustrate how progressive stages of CSD analysis enhance the spatial localization of the evoked response. Sinks are peaks and sources are valleys. Lower right: Magnified view of the localized, evoked current sink (excitatory synaptic drive). Note the lateral sources and the dorsal shift in sink location at 29 ms.

separation equal to the increment between recording locations. These functions represent the direction (positive or negative deflection) and density (absolute magnitude) of current flowing towards or away from the recording sites. Since we have not actually measured the tissue conductance in gerbil IC, current densities are expressed in arbitrary units.

The upper right plot (Fig. 1, 'Current Source Density') shows the second spatial derivatives, $F''(x) = d^2V/dx^2$. This representation of the data illustrates the distribution of sources and sinks, in both space and time, that are evoked across a linear dimension in the IC. In this figure current sinks are represented by peaks and current sources

by valleys. This step-by-step illustration of CSD analysis is presented to show that each successive derivative enhances local activity and eliminates distant, volume-conducted responses. For example, a 7 ms latency peak extending across the length of the penetration is seen in the voltage plots. Since the onset peak in the evoked potential data is approximately constant with respect to distance, both its 1st and 2nd derivatives are nearly zero. This indicates that only a small proportion is generated locally.

The bottom right plot is an enlarged view of the current sink maximum at 21.5 ms (excitation) located between 1.7 and 1.9 mm. The most striking feature of this component is that it represents

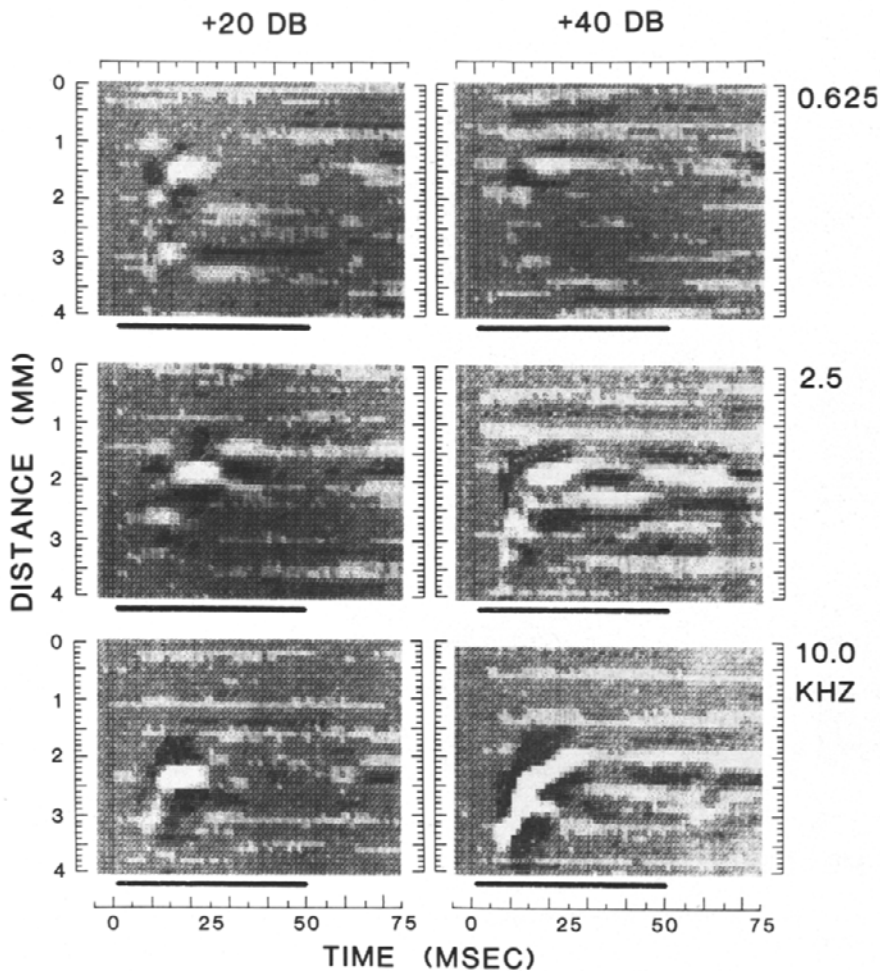


Fig. 2. CSD plots for animal G80 evoked by six different stimuli. A two octave shift in stimulus frequency is associated with a spatial shift in the evoked sink of $400 \mu\text{m}$ from 0.625 to 2.5 kHz and $500 \mu\text{m}$ from 2.5 to 10 kHz. This electrode penetration was made in the sagittal plane 1.4 mm lateral. It was not exactly aligned with the tonotopic axis as indicated by the small low frequency response.

a highly localized current sink with adjacent current sources. In the temporal dimension the onset peak is followed by a similar localized source while activity shifts spatially to establish a steady-state sink at 1.5 mm. The transient sink also has this basic conformation when evoked by a 10 kHz or 625 Hz tone-burst. However, the response becomes more complex at 625 Hz and at higher stimulus levels (Figs. 2, 3).

The most obvious result of changing stimulus frequency is the spatial shift in the evoked response. This is clearly illustrated in Figs. 2 and 3 where the data are displayed in a format that

facilitates quantitative analysis. Time is represented along the x-axis, distance along the y-axis (top dorsal) and current sink (white) and source (black) densities are represented by shades of gray. In these figures, the CSD plots have been arranged according to frequency (0.625, 2.5, and 10 kHz) and level (20 and 40 dB above AP threshold). For animal G80, peaks are evoked at 1.5, 1.9, and 2.4 mm for the 0.625, 2.5, and 10 kHz tones, respectively. This represents a shift of $225 \mu\text{m}/\text{octave}$. A similar relationship exists in the data for animal G92 shown in Fig. 3. Here the distance/frequency shift is $275 \mu\text{m}/\text{oct}$. For all seven animals the

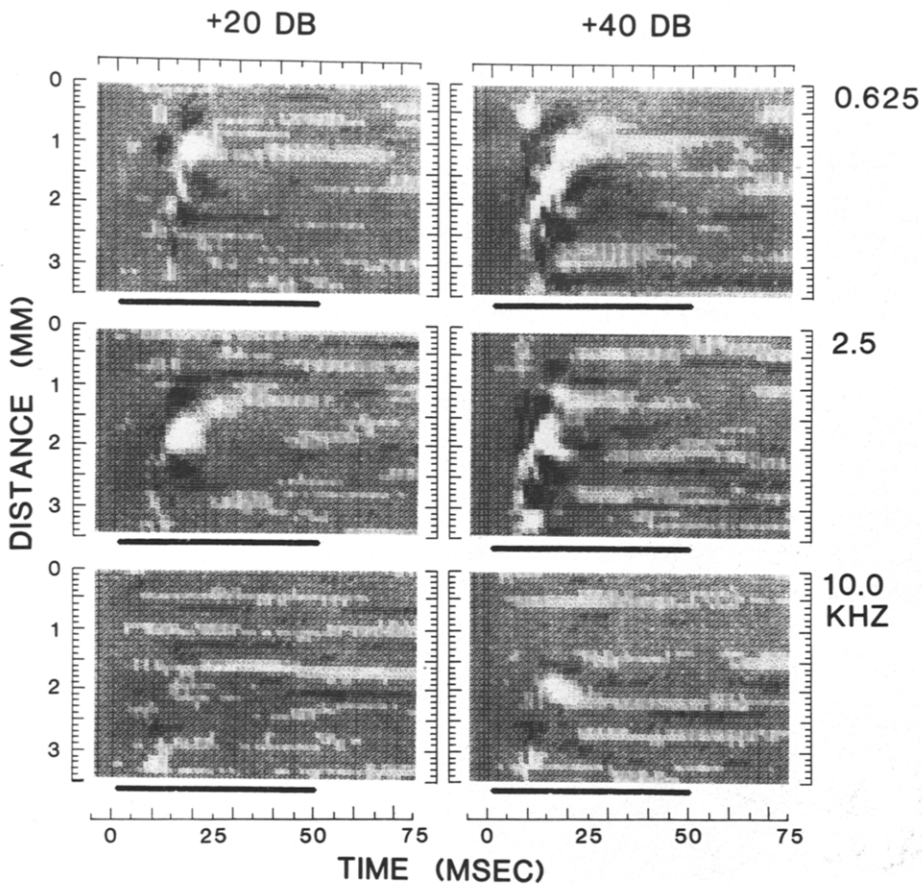


Fig. 3. CSD plots for animal G92. Conditions were identical to those for animal G80 (Fig. 2) except the penetration was more lateral at 1.8 mm. Notice the smaller high frequency response.

median shift was $280 \mu\text{m}/\text{oct}$ with a range of $210\text{--}340 \mu\text{m}/\text{oct}$. All electrode penetrations were in approximately the same location.

The location/frequency data for animal G80 have been superimposed on the electrode track reconstructed in Fig. 4. The cochlea of this animal has also been reconstructed and is shown in both sagittal and coronal projections. We have indicated the approximate best frequency location on the spiral for our stimuli as gleaned from the map of Schmiedt and Zwislocki, 1977.

Discussion

This method of analysis illustrates the tonotopic shift expected in the IC. Since the range of hearing in the gerbil is about 10 oct ($50 \text{ Hz}\text{--}60 \text{ kHz}$) (Ryan, 1976), and the spatial shift measured

is $280 \mu\text{m}/\text{oct}$, this range translates into a distance of 2.8 mm to represent the entire hearing range. This simple calculation agrees with the approximate length of the long dimension of the central nucleus of the gerbil IC. An obvious spatial compression occurs between the frequency map along the basilar membrane (adult length 11–13 mm) and its representation in IC (approximately 3 mm).

It is assumed that the orientation shown in Fig. 4 is an approximation of the tonotopic axis in the sagittal plane (Clopton and Winfield, 1973; Ryan et al., 1982). However, there is also an angle to the axis in the lateral-medial plane. That is, the tonotopic axis courses from the low frequency, dorsal pole of IC in an anterior-ventral-medial direction. This is indicated by the data shown in Figs. 2 and 3. In animal G80, the penetration was 1.4 mm

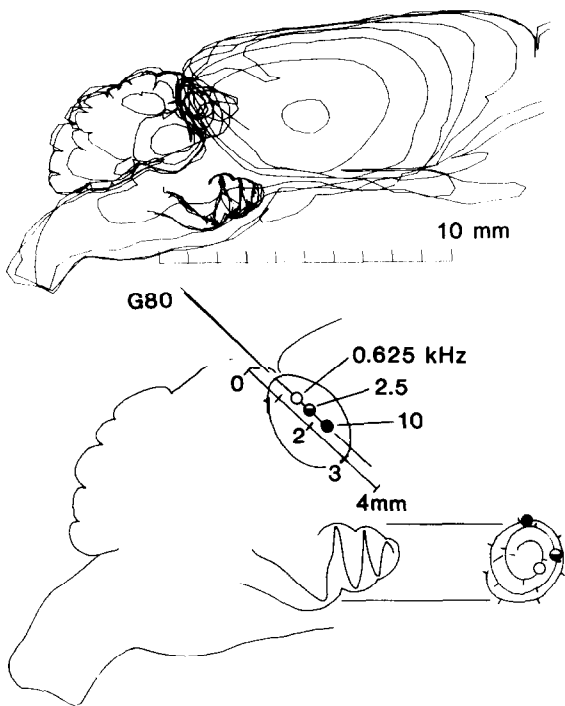


Fig. 4. Computer-assisted reconstruction of the brain, inferior colliculus, electrode track and cochlea of animal G80. The location of the current sink evoked by 0.625, 2.5, and 10 kHz tones is plotted along the distance scale through inferior colliculus. The location of these frequencies on the cochlear spiral is estimated from the map of Schmiedt and Zwislocki (1977).

lateral to the midline (λ). As shown by an attenuated response to the 0.625 kHz tone, this recording track apparently missed the low frequency portion of IC. The penetration in G92 was more lateral (1.8 mm) and appears to have missed the high frequency, ventral-medial portion of IC. These data are consistent with the tilted iso-frequency contours described in the IC by others.

Many central auditory pathway frequency maps are one-dimensional (e.g. Rose et al., 1963; Merzenich and Reid, 1974), corresponding with cochlear frequency maps. This ignores temporal information, spatial information of the single, one-dimensional axis of the penetration, response amplitude information and the spatial profile of activity evoked by specific tones. Across-fiber studies add information about the temporal response patterns and the spatial amplitude profile.

Across-fiber patterns have been reconstructed for the auditory nerve from single fiber data (Kiang, 1975; Kim and Molnar, 1979; Sachs and Young, 1979; Delgutte, 1980) and from AP data (De Boer, 1975; Ozdamar and Dallos, 1976; Elberling, 1977; Antoli-Candela and Kiang, 1978) but across-neuron patterns have not been reconstructed in the central auditory pathway. Two indirect methods for determining these patterns have been developed. The patterns of uptake of 2-deoxyglucose following acoustic stimulation demonstrate the spatial profile of tone-evoked activity (Ryan et al., 1982) and CSD analyses outline the across-neuron patterns as well as providing information about the temporal characteristics of the responses (Muller-Preus and Mitzdorf, 1984; and this study).

Current sinks are established when membrane depolarization causes ionic currents to flow into a neuron. The current sinks evoked in IC by tonal stimuli could be the result of synchronous synaptic input generating excitatory post-synaptic potentials (epsp's) in a circumscribed population of neurons. Current sinks are commonly equated with excitatory synaptic drive. Adjacent current sources, then, represent passive loop closing currents. However, current sources may also be generated by inhibitory post-synaptic activity (ipsp's) with associated, passive, loop-closing current sinks. These alternatives cannot be distinguished from CSD analyses alone.

It is instructive to inquire if the CSD response is a reasonable estimate of the spatial extent of tone-burst-evoked activity. A modeling method was developed by Ozdamar and Dallos (1976) to compare N_1 responses (population response) with single auditory nerve fiber responses. It is used here to generate a similar description for central population responses comparing CSD functions with model 'across-neuron tuning curves.' The median Q_{10} 's of a sample of single neuron tuning curves recorded from adult gerbil IC (Semple and Kitzes, 1985) are used to construct 'typical' IC tuning curve tips (Fig. 5, FTCs). In this simple model differences in unit thresholds are ignored. Also ignored is the heterogeneity in sharpness and shape that characterizes IC tuning curves. From the family of simplified tuning curves we can identify graphically the extent of best frequencies of the population of neurons that are excited by a

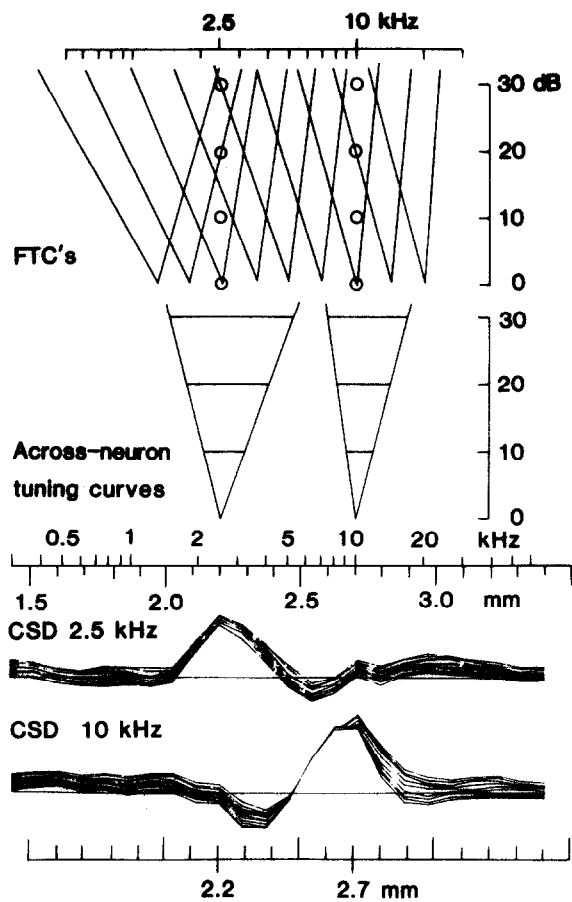


Fig. 5. Comparison of single neuron with CSD data. At the top are a family of idealized tuning curve (FTC) tips based on published data (Semple and Kitzes, 1985) from single cell recordings in the central nucleus of the inferior colliculus of adult gerbils. From this family of FTCs two across-neuron tuning curves are constructed according to the method of Ozdamar and Dallos (1976) and as described in the text. For a specific stimulus frequency, here 2.5 and 10 kHz, the across-neuron curves indicate the level-dependent spread of excitation to fibers tuned to more distant frequencies. The frequency scale is aligned with the distance scale according to the $250 \mu\text{m}/\text{octave}$ shift of the evoked current sink. For comparison the CSD functions around the latency of the maximum evoked current sink (2.5 and 10 kHz, +20 dB) are plotted at the bottom. Both the across-neuron model and the CSD functions indicate a similar population of neurons excited by the two stimuli.

fixed frequency tone at various intensities. For example, 2.5 kHz will excite, at threshold, only neurons tuned to 2.5 kHz. Raising the intensity to +10 dB will excite a restricted population of cells

that are tuned between 2.2 and 3.1 kHz, and at +20 dB the population of excited neurons expands to encompass those with best frequencies from 1.7 to 3.6 kHz. These frequency ranges plotted at the appropriate level define the across-neuron tuning curve for a 2.5 kHz tone (Fig. 5). A similar curve has been constructed for a 10 kHz tone.

Since it is known that the excitatory response is centered at a specific location for 0.625, 2.5, and 10 kHz, then there is a basis for aligning the distance axis from the CSD maps to the frequency scale of the across-neuron model. Here we assume a linear relationship between log frequency and distance.

Plotted in Fig. 5 for comparison is the CSD profile at the latency of the peak current sink evoked by a 2.5 kHz +20 dB tone-burst. Positive CSD values, indicating local excitatory input, subtend a distance of $400 \mu\text{m}$ (2.0–2.4 mm depth). The across-neuron model predicts that a +24 dB tone would excite this same population in both location and extent. Given that the CSD stimulus was calibrated re AP threshold and that AP threshold is about 5 dB less sensitive than unit thresholds (Dallos et al., 1978; Harris, 1979) then this is in reasonable agreement. The CSD response also shows a spatial asymmetry that corresponds to a high/low frequency asymmetry of the across-neuron model. The 10 kHz data do not correlate as well since the model predicts a 25% narrower ensemble than is actually obtained from the CSD analysis.

The CSD functions illustrated in Fig. 5 represent the IC onset response. This component appears to be broader and located more ventrally than the steady-state response. The steady-state component often shows multiple peaks and valleys that become more prominent at higher stimulus levels (Fig. 2, +40 dB). In some cases, the steady-state profile shows alternate banding of sources and sinks. These multiple bands, apparent in the steady-state response, are similar to the banding patterns produced in gerbil IC in stimulus-induced 2-deoxyglucose labelling experiments (Ryan et al., 1982).

CSD analysis represents a global perspective of auditory physiology. The surfaces plotted in Figs. 1–3 give the overall temporal and spatial pattern

of activity evoked in IC, and as such, provide a general context for understanding single unit data. In this case the direct measurement of population variables provides organizing information about elements not available from examination of the elements themselves. That is, it may be of use to examine details (single unit activity) from a top-down perspective as an alternative to trying to reconstruct, from the bottom-up, the overall pattern from a large and variable sample of unit responses.

Acknowledgements

This research is supported by NIH Grant NS 19518. The author would like to thank David Goodman and David Lambert for their comments on the manuscript, Cindy Smith and Glenn Krol for their technical assistance, as well as Dorothy Volk and Tina Tiffin for preparation of the manuscript.

References

- Aitkin, L.M., Webster, W.R., Veale, J.C. and Crosby, D.C. (1975) Inferior colliculus. I. Comparison of response properties of neurons in central, pericentral and external nuclei of adult cat. *J. Neurophysiol.* 38, 1196–1207.
- Antoli-Candela, F. Jr. and Kiang, N.Y.-S. (1978) Unit activity underlying the N_1 potential. In: *Evoked Electrical Activity in the Auditory Nervous System*, pp. 165–191. Editors: R.F. Naunton and C. Fernandez. Academic Press, New York, London.
- Clopton, B.M. and Winfield, J.A. (1973) Tonotopic organization in the inferior colliculus of the rat. *Brain Res.* 56, 355–358.
- Creutzfeldt, O.D., Watanabe, S. and Lux, H.D. (1966) Relations between EEG phenomena and potentials of single cortical cells. I. Evoked responses after thalamic and epicortical stimulation. *Electroencephalogr. Clin. Neurophysiol.* 20, 1937.
- Creutzfeldt, O.D., Rosina, A., Ito, M. and Probst, W. (1969) Visual evoked response of single cells and of the EEG in primary visual area of the cat. *J. Neurophysiol.* 32, 127–139.
- Dallos, P., Harris, D., Ozdamar, O. and Ryan, A. (1978) Behavioral compound action potential and single unit thresholds: Relationship in normal and abnormal ears. *J. Acoust. Soc. Am.* 64, 151–157.
- De Boer, E. (1975) Synthetic whole nerve action potentials for the cat. *J. Acoust. Soc. Am.* 58, 1030–1045.
- Delgutte, B. (1980) Representation of speech-like sounds in the discharge patterns of auditory-nerve fibers. *J. Acoust. Soc. Am.* 68, 843–857.
- Elberling, C. (1977) Deconvolution of action potentials recorded from the ear canal in man. In: *Disorders of Auditory Function II*. Editor: S.D.G. Stephens. Academic Press, New York.
- Elul, R. (1964) Specific site of generation of brain waves. *Physiologist* 7, 125.
- Elul, R. (1974) Relation of neuronal waves to EEG. In: *Dynamic patterns of brain cell assemblies*. NRP Bull. 12, 97–101.
- Evans, E.F. and Nelson, P.G. (1973) The response of single neurons in the cochlear nucleus of the cat as a function of their location and the anesthetic state. *Exp. Brain Res.* 17, 402–427.
- Freeman, J.A. and Nicholson, C. (1975) Experimental optimization of current source-density technique for anuran cerebellum. *J. Neurophysiol.* 38, 369–382.
- Freeman, B. and Singer, W. (1983) Direct and indirect visual inputs to superficial layers of cat superior colliculus: a current source-density analysis of electrically evoked potentials. *J. Neurophysiol.* 49, 1075–1091.
- Gerstein, G.L. (1970) Functional association of neurons: detection and interpretation. In: *The Neurosciences Second Study Program*, pp. 648–660. Editor: F.O. Schmitt. Rockefeller Univ. Press.
- Hamming, R.W. (1962) *Numerical Methods for Scientists and Engineers*. McGraw, New York.
- Harris, D.M. (1979) Action potential suppression, tuning curves and thresholds: Comparison with single fiber data. *Hear. Res.* 1, 133–154.
- Harris, D.M. and Riera-March, A. (1985) Spatial patterns of synaptic input in inferior colliculus. Eighth Midwinter Res. Meet. Assoc. Res. Otolaryngol.
- Harris, D.M. and Rosenfeld, J.P. (1975) Frequency analysis by neuronal populations in the inferior colliculus of the rat. *J. Acoust. Soc. Am.* 57, S53–54.
- Howland, B., Lettvin, J.Y., McCulloch, W.S., Pitts, W. and Wall, P.D. (1955) Reflex inhibition by dorsal root interaction. *J. Neurophysiol.* 18, 1–17.
- John, E.R. (1972) Switchboard versus statistical theories of learning and memory. *Science* 177, 850–864.
- Kiang, N.Y.-S. (1975) Stimulus representation in the discharge patterns of auditory neurons. In: *The Nervous System*, Vol. 3, pp. 81–96. Editor: E.L. Eagles. Raven Press, New York.
- Kim, D.O. and Molnar, C.E. (1979) A population study of cochlear nerve fibers: Comparisons of the spatial distributions of average-rate and phase locking measures of responses to single tones. *J. Neurophysiol.* 42, 16–30.
- Lorente de No, R. (1947) *A Study of Nerve Physiology*. Chapter XVI. Rockefeller Inst. Med. Res., New York.
- Manis, P.B. and Brownell, W.E. (1983) Synaptic organization of eighth nerve afferents to cat dorsal cochlear nucleus. *J. neurophysiol.* 50, 1156–1181.
- Merzenich, M.M. and Reid, M.D. (1974) Representation of the cochlea within the inferior colliculus of the cat. *Brain Res.* 77, 397–415.
- Mitzdorf, U. and Singer, W. (1977) Laminar segregation of afferents to lateral geniculate nucleus of the cat: an analysis of current source density. *J. Neurophysiol.* 40, 1227–1243.
- Mitzdorf, U. and Singer, W. (1979) Excitatory synaptic ensemble properties in the visual cortex of the macaque monkey:

- a current source density analysis of electrically evoked potentials. *J. Comp. Neurol.* 187, 71–84.
- Mitzdorf, U. and Singer, W. (1980) Monocular activation of visual cortex in normal and monocularly deprived cats: an analysis of evoked potentials. *J. Physiol.* 304, 203–220.
- Muller-Preus and Mitzdorf, U. (1984) Functional anatomy of the inferior colliculus and the auditory cortex; current source density analyses of click-evoked potentials. *Hear. Res.* 16, 133–142.
- Nicholson, C. (1973) Theoretical analysis of field potentials in anisotropic ensembles of neuronal elements. *IEEE Trans. Biomed. Engineer.* Vol. BME-20, No. 4, 278–288.
- Nicholson, C. and Freeman, J.A. (1975) Theory of current source-density analysis and determination of conductivity tensor for anuran cerebellum. *J. Neurophysiol.* 38, 356–368.
- Nicholson, C. and Llinas (1971) Field potentials in alligator cerebellum and theory of their relationship to Purkinje cell dendritic spikes. *J. Neurophysiol.* 34, 509–531.
- Ozdamar, O. and Dallos, P. (1976) Input-output functions of cochlear whole-nerve action potentials. Interpretation in terms of one population of neurons. *J. Acoust. Soc. Am.* 59, 143–147.
- Perkel, D.H. and Bullock, T.H. (1968) Neural Coding. *Neurosciences Res. Prog. Bull.* 6.
- Pitts, W. (1952) Investigations on synaptic transmission. *Cybernetics Trans.* 9th Conf. 159–166.
- Purpura, D.F. (1959) Nature of electrocortical potentials and synaptic organizations in cerebral and cerebellar cortex. *Intern. Rev. Neurobiol.* 1, 47–163.
- Rall, W. (1967) Distinguishing theoretical synaptic potentials computed for different soma-dendritic distributions of synaptic input. *J. Neurophysiol.* 30, 1139–1168.
- Rockel, A.J. and Jones, E.G. (1972) The neuronal organization of the inferior colliculus of the adult cat. I. The central nucleus. *J. Comp. Neurol.* 147, 11–60.
- Rose, J.E., Greenwood, D.D., Goldberg, J.M. and Hind, J.E. (1963) Some discharge characteristics of single neurons in the inferior colliculus of the cat. I. Tonotopic organization, relation of spike-counts to tone intensity and firing patterns of single elements. *J. Neurophysiol.* 26, 294–320.
- Roth, G.L., Aitkin, L.M., Andersen, R.A. and Merzenich, M.M. (1978) Some features of the spatial organization of the central nucleus of the inferior colliculus of the cat. *J. Comp. Neurol.* 182, 661–680.
- Ryan, A. (1976) Hearing sensitivity of the mongolian gerbil, *Meriones unguiculatis*. *J. Acoust. Soc. Am.* 59, 1222–1226.
- Ryan, A.F., Woolf, N.K. and Sharp, F.R. (1982) Tonotopic organization in the central auditory pathway of the mongolian gerbil: A 2-deoxyglucose study. *J. Comp. Neurol.* 207, 369–380.
- Sachs, M.B. and Young, E. (1979) Encoding of steady state vowels in the auditory nerve: Representation in terms of discharge rate. *J. Acoust. Soc. Am.* 66, 470–479.
- Schmiedt, R.A. and Zwislocki, J.J. (1977) Comparison of sound-transmission and cochlear-microphonic characteristics in Mongolian gerbil and guinea pig. *J. Acoust. Soc. Am.* 61, 133–149.
- Semple, M.N. and Aitkin, L.M. (1979) Representation of sound frequency and laterality by units in central nucleus of cat inferior colliculus. *J. Neurophysiol.* 42, 1626–1639.
- Semple and Kitzes (1985) Single-unit responses in the inferior colliculus: Different consequences of contralateral and ipsilateral auditory stimulation. *J. Neurophysiol.* 53, 1467–1482.